Cathodic Elimination Reactions of Acyclic Vicinal Dibromides

Oliver R. Brown and Peter H. Middleton
Department of Physical Chemistry, The University, Newcastle upon Tyne
Terence L. Threlfall
May and Baker Ltd., Dagenham, Essex

Electrochemical reductions of both *meso*- and DL-isomers of 3,4-dibromohexane and 2,5-dimethyl-3,4-dibromohexane have been carried out on various cathodes in ammonia and in DMF solvent systems in order to measure reduction potentials and to determine product distributions. The *cis*/*trans* ratios of the products hex-3-ene or 2,5-dimethylhex-3-ene varied with electrode potential in most cases. *anti*-Elimination of two bromide ions by a concerted mechanism occurred preferentially except in the icase of DL-2,5-dimethyl-3,4-dibromohexane which was unable to attain the *anti*-configuration. At sufficiently negative potentials all rotamers were reduced under diffusion control such that the product distribution reflected the distribution of conformers in the reactant. In liquid ammonia the product yields at negative potentials were similar for *meso*- and DL-reactants as reduction by solvated electrons proceeded stepwise through an intermediate which can undergo free rotation. Appendices are included which describe calculations of (1) the intramolecular van der Waals contributions to the conformational energies of the reactant dibromides and (2) distances of electron transfer from cathodes to diffusion-controlled depolarisers when the tunnelling barrier is rectangular.

Electrochemical reductions of vicinal dibromides usually lead mainly to olefins.[1-5] A single polarographic wave is commonly obtained at an electrode potential more positive than the $E_{\frac{1}{2}}$ of the corresponding monobromides, indicating that elimination of both bromide ions occurs either as a concerted process or as two events in quick succession. In the cathodic eliminations of the 2,3-dibromobutanes, the DL-isomer was reported to give only *cis*-butene and the *meso*-compound afforded exclusively *trans*-butene.[3] Measurements of $E_{\frac{1}{2}}$ of various rigid cyclic vicinal dibromides in which the stagger, or dihedral, angle θ ranged from 0 to 180° showed that reduction was easiest when θ = 180° and most difficult when θ = 90°; *syn*-elimination was of intermediate difficulty.[4]

trans-1,2-Dibromocyclohexane, at room temperature, gave a single cyclic voltammetric peak but, at progressively lower temperatures, the height decreased as, at more negative potentials, a second peak grew.[5a] It is believed that the reduction proceeded preferentially through the *anti*- (axial, axial) conformer so long as equilibrium with the less easily reduced *gauche* (equatorial, equatorial) conformer could be maintained ($\Delta G^{0\ddagger}$ 46 kJ mol^{-1}).[5] Recently that work was extended to include substituted 1,2-dibromocyclohexanes and some acyclic vicinal dibromides.[5b] Rate constants and equilibrium constants were evaluated for some conformer interconversions. However, even at −135 °C, the conformers of each isomer of 2,3-dibromobutane remain in equilibrium whereas, in contrast, at temperatures as high as 80 °C both isomers of 3,4-dibromo-2,5-dimethylhexane exist as only a single conformation. Using classical polarography, Feoktistov and Gol'din found that different rotameric forms of 1,2-dibromoperfluoroethane were reduced to distinctly different products.[6-8]

Chemical reductions by reagents which transfer electrons singly proceed *via* radical intermediates to mixtures of *cis*- and *trans*-olefins.[9,10] In systems where suitable substituents enable the intermediate radicals to be stabilised by delocalisation of the unpaired electron, even cathodic reductions yield *cis*/*trans* mixtures whose composition depends upon the medium (pH, nature, and concentration of cations).[11,12] The present work concerns vicinal dibromides which are not expected to produce stable radicals. Neither are they expected to undergo loss of bromide ions singly. Furthermore, equilibrium between rotamers is expected to be easily maintained. Therefore the products are expected to be olefins, whose relative amounts will not be indicated by amperometric measurements; instead chemical analysis will be required.

$CH_3CHRCHBrCHBrCHRCH_3$
(1) R = H
(2) R = CH_3

$CH_3CHRCH{=}CHCHRCH_3$
(3) R = H
(4) R = CH_3

When the solvent used for the electrolysis is liquid ammonia or a lower aliphatic amine, then increasing the electrode potential in a negative direction might promote a change in product distribution as a result of a change from a conventional two-electron cathodic reduction to one-electron reduction through the intermediacy of solvated electrons. An analogous interception of reactants, *en route* to the electrode, by reactive electro-generated species has been reported previously for the anodic chlorination of cyclohexene.[13] The model dibromides used for this investigation are 3,4-dibromohexane (1) and 2,5-dimethyl-3,4-dibromohexane (2). The products of cathodic elimination are respectively hex-3-ene (3) and 2,5-dimethylhex-3-ene (4).

Results

The DL- and *meso*-forms of compounds (1) and (2) were reduced at the dropping mercury electrode (DME) and at stationary platinum wire electrodes in *NN*-dimethylformamide (DMF) solutions (0.4M-tetrabutylammonium tetrafluoroborate, TBAF). In the case of (1), cathodes of gold, amalgamated copper, and vitreous carbon were also used for linear potential sweep amperometry. In all cases, single irreversible waves were observed on fresh clean electrodes. Measured $E_{\frac{1}{2}}$ or $E_{p/2}$ potentials are presented in Table 1. In general *meso*-isomers were reduced more readily than the corresponding DL-form; in the case of (1) the difference in $E_{\frac{1}{2}}$ was only some 0.2 V but for (2) the difference was of the order of 1 V. Comparisons of the diffusion current constants obtained using

Table 1. Electrode potential data for reductions of compounds (1) and (2) in DMF solutions

			meso-Isomer		DL-Isomer	
Compound	Electrode	Parameter	Most positive value (V)	Mean value (V)	Most positive value (V)	Mean value (V)
(1)	DME	$E_{\frac{1}{2}}$	−0.860	−0.860	−1.070	−1.070
(1)	Platinum	$E_{p/2}$	−0.530	−0.550	−0.480	−0.685
(1)	Gold	$E_{p/2}$	−0.420	−0.450	−0.730	−0.730
(1)	Cu amalgam	$E_{p/2}$	−0.880	−0.880	−1.070	−1.070
(1)	Carbon	$E_{p/2}$	−0.590	−0.590	−1.300	−1.300
(2)	DME	$E_{\frac{1}{2}}$	−0.810	−0.810	−1.605	−1.605
(2)	Platinum	$E_{p/2}$	−0.350	−0.350	−1.870	−1.870

Table 2. Electrode potential data for the reductions of compounds (1) and (2) in liquid ammonia solutions

			meso-Isomer		DL-Isomer	
Compound	Electrode	Parameter	Most positive value (V)	Mean value (V)	Most positive value (V)	Mean value (V)
(1)	Platinum	$E_{p/2}$	0.004	−0.062	−0.080	−0.089
(1)	Gold	$E_{p/2}$	−0.060	−0.081	−0.060	−0.109
(1)	Carbon	$E_{p/2}$	−1.240		beyond −1.240	
(2)	Platinum	$E_{p/2}$	−0.060	−0.207	−0.340	−0.412
(2)	Gold	$E_{p/2}$	−0.035	−0.053	−0.670	−0.695
(2)	Carbon	$E_{p/2}$			−1.165	

the DME with literature values for known reactions involving molecules of similar size in DMF indicated that the charge being transferred was 2 F mol^{-1}.

Amperometric examinations were made of all four dibromides in liquid ammonia solutions (0.5M-KBr) with cathodes of Pt, Au, and vitreous carbon. Results obtained with this solvent were generally much less reproducible and sometimes, upon repeated scanning of potential, the current peak observed on platinum degenerated into a pair of peaks. Increased additions of the co-solvent, tetrahydrofuran (THF), did not alleviate this problem but generation of solvated electrons by potential excursions beyond −1.9 V for a few seconds caused revitalisation of the cathode, manifested by a positive shift in E_p of the dibromide peak on subsequent scans. Gold cathodes behaved more reproducibly than platinum but they too benefited from *in situ* reactivation: not by cathodic treatment which would have led to dissolution of the metal,[14] but instead by anodic polarisation at +1.2 V. Table 2 lists the reduction potentials recorded using ammonia solutions. Again the *meso*-isomers tended to be reduced more readily than their DL counterparts but the effect was less pronounced than in DMF. Vitreous carbon showed a remarkable lack of activity under these conditions.

Controlled-potential electrolyses with coulometry were performed using various cathode materials and electrode potentials ranging from $E_{p/2}$ to the cathodic limit of the solvent. Compound (2) was studied only in ammonia solutions. In DMF solutions compound (1) behaved stereospecifically at less negative reduction potentials; the *meso*-dibromide afforded exclusively *trans*-alkene whereas the DL-isomer gave 97% *cis*-hex-3-ene (the discrepancy from 100% can be ascribed to the presence of a small amount of *meso*-impurity in the reactant). Figure 1 shows that, as the reduction potential was made progressively more negative, stereospecificity was gradually lost and a limiting behaviour, obtained at sufficiently negative potentials, corresponded to a *cis* : *trans* product distribution of 50 : 50 from *meso*-(1) and 30 : 70 from the DL-isomer.

When liquid ammonia was used as the solvent, (1) showed stereospecific behaviour at the positive end of the reduction

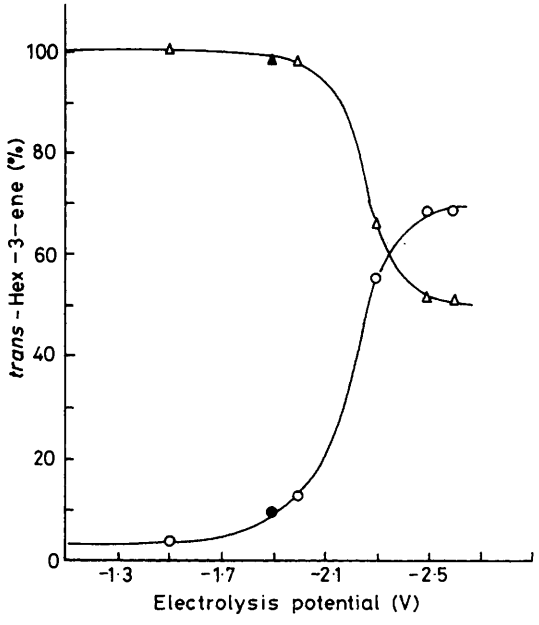

Figure 1. Distribution of products, *cis*- and *trans*-hexene, obtained at mercury pool (filled symbols) and platinum sheet (empty symbols) cathodes in DMF–0.4M-TBAF during controlled-potential electrolyses of 3,4-dibromohexane (△, ▲ *meso*-isomer; ○, ● DL-isomer)

range, similar to that found when DMF was used as the solvent. Furthermore, as the potential was made more negative the stereospecificity was gradually lost but the form of the dependence of product yields upon electrode potential differed from that found in DMF. Figures 2 and 3 display the behaviours observed with platinum and gold cathodes respectively. On platinum, where the potential region corresponding to the formation of solvated electrons is accessible, the product distribution at the negative limit was independent

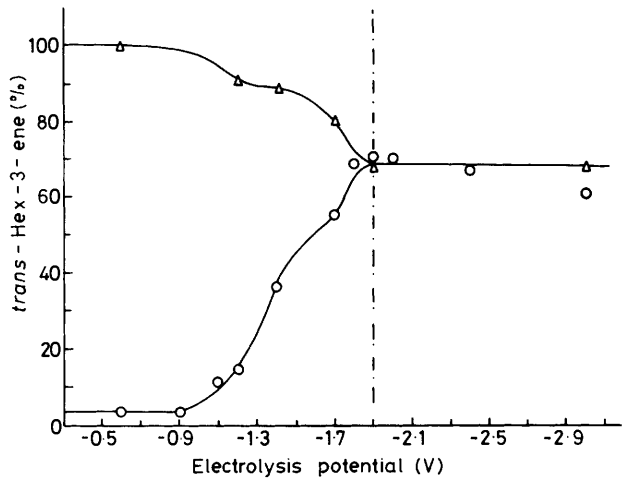

Figure 2. Distribution of products, *cis*- and *trans*-hex-3-ene, obtained at platinum cathodes in liquid ammonia–10% THF–0.5M-KBr during controlled-potential electrolyses of 3,4-dibromohexane at −40 °C (△ *meso*, ○ DL)

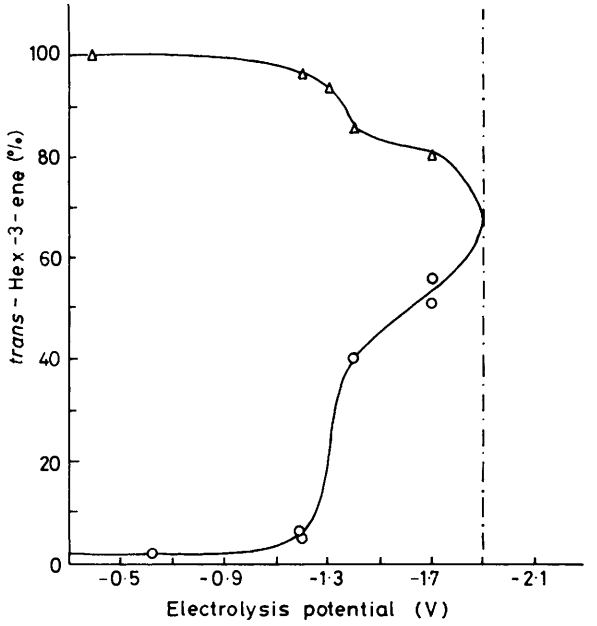

Figure 3. Distribution of products, *cis*- and *trans*-hex-3-ene, obtained at gold cathodes in liquid ammonia–10% THF–0.5M-KBr during controlled-potential electrolyses of 3,4-dibromohexane at −40 °C (△ *meso*, ○ DL)

of the isomer used as reactant; a *cis* : *trans* ratio for hex-3-ene was found to be 31 : 69 whether the reactant was *meso*-(1) or DL-(1).

The possibility of isomerisation taking place between the *cis*- and *trans*-hex-3-ene products in the strongly reducing conditions afforded by alkali metal–ammonia solutions was examined. A sample of *cis*-hex-3-ene was added to a stirred bronze-coloured solution of sodium (3.5 mol dm^{-3}) in ammonia in contact with liquid butane at −40 °C, a two-phase system in which we have performed several reductions by solvated electrons. After 9 h the excess of alkali metal was quenched and hex-3-ene analysed. *trans*-Hex-3-ene was found only in the small amount (3%) corresponding to that initially present as an impurity in *cis*-hex-3-ene.

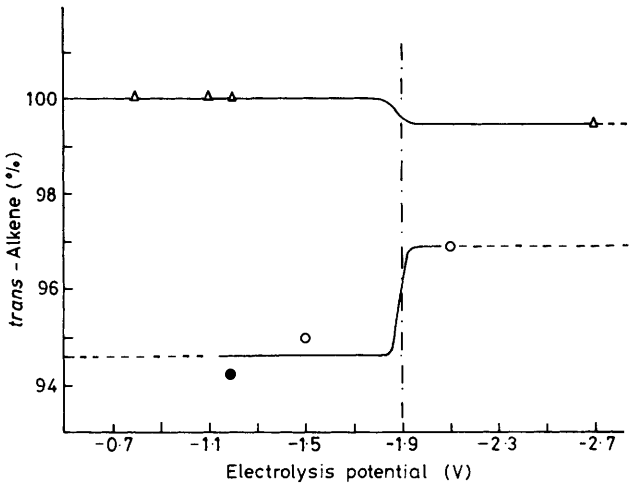

Figure 4. Distribution of products, *cis*- and *trans*-2,5-dimethylhex-3-ene, obtained at gold (filled symbols) and platinum (empty symbols) cathodes in liquid ammonia–10% THF–0.5M-KBr during controlled-potential electrolyses of 2,5-dimethyl-3,4-dibromohexane at −40 °C (△, ▲ *meso*; ○, ● DL)

Compound (2) exhibited quite different behaviour; the *meso*-form gave exclusively *trans*-2,5-dimethylhex-3-ene under conditions of direct cathodic reduction where the DL-isomer yielded a *cis* : *trans* product ratio of 5 : 95. In the solvated electron region the *trans*-olefin remained predominant (Figure 4).

During controlled-potential electrolyses in ammonia, the logarithms of the currents fell linearly with time [except occasionally when *meso*-(2) was reduced on platinum]; in every case 2 F mol^{-1} was consumed. A similar coulometric result was obtained with DMF as solvent, but the log *I* *versus* *t* relationship was distorted as a result of the temperature rise within the unthermostatted cell.

Discussion

The stereospecificity observed for the reduction of (1) under mild potential conditions is consistent with the well established view that conformers in which the bromine atoms are *anti* are able to undergo elimination reactions more readily than are their *syn* counterparts (Scheme). The small difference in $E_{\frac{1}{2}}$ between the reduction potentials of the two isomers can be ascribed to the greater difficulty with which the DL-form can achieve the *anti*-conformation, resulting from interactions between ethyl groups. The calculations of strain energies of the various rotamers (Appendix 1) indicate that the *anti*-conformers are not the most stable rotamers either for the *meso*- or DL-isomers. However, *meso*-(1) requires only some 8 kJ mol^{-1} to form the *anti*-arrangement whereas DL-(1) needs *ca.* 20 kJ mol^{-1} (based upon calculation of intramolecular van der Waals interactions only).

In all cases, analyses of the shapes of the experimental polarisation curves (current *versus* electrode potential data) showed the reduction rates to exhibit a low dependence on electrode potential. Low transfer coefficients (*i.e.* high values for the Tafel slopes) are indeed a characteristic of cathodic reductions of organic halides and they indicate clearly that the slow step in the reduction is the transfer of the first electron to the substrate molecule. In the case of a vicinal dibromide we can suppose that the energy level of the antibonding orbital into which the first electron is transferred is influenced by the dihedral angle between the bromine atoms

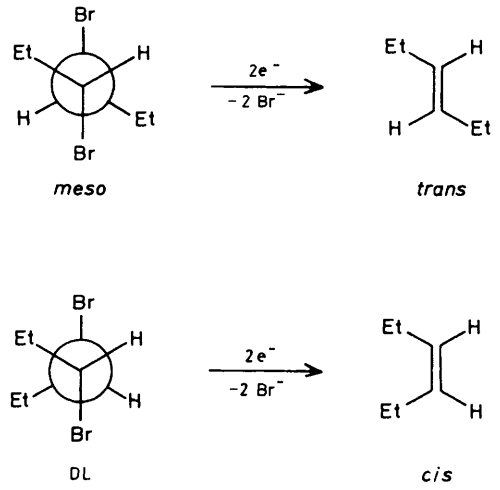

Scheme.

in the molecule; an *anti*-arrangement corresponds to the lowest energy of the transition state and in consequence species which most readily can assume an *anti*-conformation are most easily reduced. Subsequent loss of bromide and transfer of a second electron occur before significant further rotation can take place, except in the case of reduction by solvated electrons.

The observed stereospecificity corresponds with that reported by Casanova and Rogers for cathodic eliminations of the 2,3-dibromobutanes.[3] However, despite the fact that the effect of changing electrode potential was investigated in that study, no significant dependence of product distribution upon electrode potential was found. It is possible that, in that work as a result of ohmic potential drop within the electrolyte, the true range of electrode potentials investigated was much less than the authors supposed. By contrast, in the present work, the loss of specificity at negative potentials was evident and can be attributed to simultaneous reductions of *anti*- and *syn*-conformers at rates which, in the limit, reflect their relative concentrations in the bulk of the catholyte. Under sufficiently severe reduction conditions all rotamers will be reduced under total control by mass transfer. As diffusion coefficients of different rotamers are expected to be essentially identical, then there will be no departure, within the diffusion layer, from the equilibrium distribution of conformers which exists in the bulk of solution.

It might be argued that the equilibrium constant for the rotameric equilibrium in the strong electric fields which exist at the electrode surface will differ from that which pertains in the bulk of solution; the dipolar *syn*-conformation is expected to be favoured by strong fields at the expense of the quadripolar *anti*-form. There are three reasons why we believe that this effect can be discounted and we outline them below. (1) As argued by Feoktistov and Gol'din,[8] the time, τ, spent by any molecule in the vicinity of the electrode surface, say within 1.0 nm, is extremely short. The Einstein–Smoluchowski equation can be used to calculate τ from a knowledge of the diffusion coefficient D and the distance d. Setting D equal to 1×10^{-9} m^2 s^{-1} we obtain $\tau = d^2/2D = 5 \times 10^{-10}$ s. During this short period spent by the reactant within the interface, substantial rotation can occur only if the barrier to rotation is less than or comparable with RT. The calculations presented in Appendix 1 indicate activation energies for rotation of many kJ mol^{-1}.

(2) When the applied electrode potential is very negative in relation to $E_{\frac{1}{2}}$ then the electron transfer event can occur without any need for activation of the reactant molecule; the only requirement is that the molecule should approach sufficiently near to the surface so that the probability of electron tunnelling becomes high. In Appendix 2, it is argued that, under such conditions, a large proportion of the reactant molecules will be reduced before they reach the region where the electric field strength is high.

(3) In the particular systems which form the subject of the present study, the dipolar part of the dibromide molecule lies outside the double layer when the negative (bromine) end of the dipole points away from the negatively charged electrode surface. Although the potential of zero charge (p.z.c.) of the interface is unknown, there can be little doubt that it occurs at potentials more positive than those used for reduction under diffusion control. The thickness of the diffuse part of the double layer is expressed as the Debye length (K^{-1}) which can be calculated using the relation $K = (2n^0z^2e^2/\varepsilon\varepsilon_0kT)^{\frac{1}{2}}$ where n^0 is the concentration of ions, each of charge ze. Symbols used in the denominator have their usual meanings. For a DMF solution, 0.4M in a 1 : 1 electrolyte, the Debye length at 25 °C is 0.33 nm whereas, in the *meso*-3,4-dibromohexane molecule, oriented as described, C-3 and -4 cannot approach within 0.4 nm of the electrode surface.

The positions of the rotameric equilibria for *meso*- and DL-(1) indicated by the product distributions observed with DMF as solvent under extreme cathodic conditions are consistent with values expected from considerations of plots of strain energy *versus* dihedral angle (Appendix 1, Figures 5 and 6). When (1) was reduced on platinum or gold cathodes in ammonia solutions, the product analysis results show that, before the potential is reached where the *syn*-form can be reduced directly under diffusion control, indirect reduction by solvated electrons has already become significant. Thus, beyond −1.9 V, the potential at which the blue colour of solvated electrons can normally be seen, reduction occurs by a mechanism involving the transfer of one electron at a time; the intermediate free radical permits free rotation about the central carbon–carbon bond so that the product distribution is independent of the isomer chosen as the reactant. The greater stability of *trans*-hex-3-ene over the *cis*-isomer is evident in the observed product ratio.

In the case of compound (2), the calculations described in Appendix 1 (Figures 7 and 8), show that the strain energies of those conformers which yield *cis*-2,5-dimethylhex-3-ene are substantially higher than those of the more stable conformations which lead to the *trans*-olefin upon reduction. Thus it is to be expected that the *meso*-dibromide affords exclusively *trans*-product by *anti*-elimination of the bromide ions. More interesting is the case of DL-(2) which is unique amongst the compounds studied insofar as *anti*-elimination does not predominate under mild reduction conditions; clearly the equilibrium concentrations of those conformers which would be reduced to the *cis*-olefin are small. Consistent with this interpretation is the observation that, in DMF solutions, the potential of the reduction of DL-(2), which takes place by *syn*-elimination, is vastly more negative than that of *meso*-(2), which corresponds to *anti*-elimination. It might be expected that reduction of DL-(2) would occur by *anti*-elimination at more positive potentials by means of a rapid pre-equilibrium being maintained within the diffusion layer. However in Appendix 1 it is shown that the activation energy for the conversion of *syn*-DL-(2) into *anti*-DL-(2) is very much higher than for the corresponding conversions in the other three dibromides which were studied. It is probable, therefore, that equilibrium cannot be maintained between the various rotameric forms of DL-(2). This view is in accord with that of O'Connell and Evans, based on cyclic voltammetry in butyronitrile solutions.[5a] Those authors concluded, as we do,

that *meso*-(2) exists solely as the *anti*-conformer and DL-(2) is not represented by the *anti*-form.

Our results can be discussed in terms of the Curtin–Hammett principle. Under mild reducing conditions reduction of (1) involves activation energies much larger than those required for isomerisation of rotamers. By contrast, at sufficiently negative values of electrode potential the cathodic reaction requires zero activation energy. In the case of compounds (2) the activation energy required for rotation of conformers is so large that it exceeds the activation energy for reduction at any electrode potential where detectable cathodic currents can be obtained.

The electrode potential data presented in Tables 1 and 2 exhibit several unpredictable features. In the absence of data on potentials of zero charge it is not possible to explain these effects with any certainty; it is likely that potential values are affected by inhibition phenomena resulting from the formation of polymeric films, as by-products, on the cathode surfaces. However, it is noteworthy that $E_{\frac{1}{2}}$ potentials recorded using mercury cathodes in DMF, and presumably free from films, were actually more negative than $E_{p/2}$ obtained using the transition metal electrodes Pt and Au, except in the case of DL-(2) (Table 1). This result correlates with the conclusion that DL-(2) is the only case, of the four compounds studied, in which elimination preferentially occurs by a *syn*-mechanism. If, as has often been proposed,[11,12] *anti*-elimination is a concerted process, then an electrode surface which stabilises the product olefin by interaction with its π-electrons will behave more catalytically than a surface which does not. This relative behaviour of platinum and mercury contrasts with that observed in the reductions of monobromides where mercury, with its ability to form organomercurials, appears more active than platinum cathodes.[15] The results indicate that *syn*-elimination is not a concerted process. In most cases carbon was found to be particularly inactive and it might be speculated that the surface is an especially suitable host for chemisorbed alkene products which are responsible for auto-inhibition.

The only matter of discord which exists between this work and the recent paper of O'Connell and Evans concerns the relative activities of mercury and platinum cathodes towards the reductions of antiperiplanar dibromides; those authors invariably found mercury to be the more catalytic material. Without undertaking further experimental work it is not possible to resolve this anomaly with any certainty. Although different solvent–electrolyte systems were used and the forms of the mercury cathodes differed in the two studies, substrate concentrations were similar (1.0—10mM) so there is no obvious explanation for the discrepancy.

Experimental

Measurements were made in two solvent systems, DMF, unthermostatted at room temperature, and liquid ammonia, thermostatted at −40 °C.

Equipment.—The electrochemical equipment (function generator, potentiostat, current measurement unit) were long proven designs developed in this laboratory. Elemental analysis was performed on a Carlo Erba Strumentazione MOD 1106, g.l.c. analysis on Pye 105 and F & M 810 chromatographs, ^{1}H n.m.r. spectroscopy on a variety of instruments (Bruker HFX 90, Bruker HXE 90 and Varian Anaspect EM 360), and mass spectrometry on a Kratos MS9 instrument.

Starting Materials.—In each case mass and ^{1}H n.m.r. spectra were recorded. Purity was checked by g.l.c. using two different columns; single peaks were obtained. *cis*-(4) (Pfaltz and Bauer) gave δ 1.0 (12 H, d, CH_3), 2.7 (2 H, m, >CH), and 5.1 (2 H, q, =CH), *m/e* 112 (M^+), 98, 69, 56, 55, 41, 29, and 28. *trans*-(4) (Pfaltz and Bauer) gave δ 1.0 (12 H, d, CH_3), 2.2 (2 H, m, >CH), and 5.3 (2 H, q, =CH), *m/e*, as for cis-(4). *trans*-(3) (Aldrich; gold star) gave δ 0.94 (6 H, t, CH_3), 1.98 (4 H, m, CH_2), and 5.39 (2 H, m, =CH), *m/e* 84 (M^+), 69, 55, 41, 39, 28, and 27. *Hex*-3-*yne* (Koch–Light) gave δ 1.1 (6 H, t, CH_3) and 2.14 (4 H, q, CH_2), *m/e* 82 (M^+), 53, 41, and 27.

Syntheses.—*cis*-Hex-3-ene was synthesised from hex-3-yne by catalytic hydrogenation at medium pressure on a Lindlar catalyst with toluene as solvent and quinoline as a moderator. The yield of hex-3-ene was 86% [95% *cis*-(3) and 5% *trans*-(3)] as determined by g.l.c. analysis. The ^{1}H n.m.r. spectrum had δ 0.93 (6 H, t, CH_3), 2.0 (4 H, q, CH_2), and 5.24 (2 H, sextet, =CH) and mass spectrum *m/e* 84 (M^+), 69, 55, 41, 39, 28, and 27.

meso-(2) was prepared by bromination of *trans*-(4) using the method of Schmitt and Boord [16] and Young *et al.*[17] The m.p. of the needle-like crystals was 53.0 °C, the n.m.r. spectrum had δ 0.91 (6 H, d, *J* 7 Hz, CH_3), 1.07 (6 H, d, *J* 7 Hz, CH_3), 2.5 (2 H, m, >CH), and 4.2 (2 H, s, CHBr), *m/e* 191, 147, 135, 119, 111, and 69.

DL-(2) was obtained from *cis*-(4) using the same method.[16,17] The m.p. of the plate-like crystals was 72.2 °C, the n.m.r. spectrum had δ 0.99 (6 H, d, *J* 7 Hz, CH_3), 1.14 (6 H, d, *J* 6.8 Hz, CH_3), 2.1 (2 H, m, >CH), and 3.8 (2 H, m, CHBr) and the mass spectrum *m/e* 270, 191, 147, 135, 111, and 69 (Found: C, 35.3; H, 5.9. Calc. for $C_8H_{16}Br_2$: C, 35.3; H, 5.9%). In each of these syntheses of isomers of (2) yields of crude product were 100%, falling to 50% after repeated recrystallisations from methanol at 0 °C. With the exception of the purification procedures the method of synthesis of (1) from (3) was identical.[16,17] After fractional distillations *meso*-(1) obtained from *trans*-(3) was found to be pure but DL-(1) synthesised from *cis*-(3) contained 3% *meso*-(1) as impurity, resulting from the 5% *trans*-(1) impurity in the starting material. The mass spectra of both isomers of (1) were identical, *m/e* 242 (M^+), 163, 121, and 83. The ^{1}H n.m.r. spectra were of the ABX type: *meso*-(1) had δ 1.09 (6 H, t, *J* 8 Hz, CH_3), 2.11 (4 H, sextet, CH_2), and 4.13 (2 H, m, CHBr) whereas DL-(1) had δ 1.03 (6 H, t, *J* 7 Hz, CH_3), 1.9 (4 H, m, CH_2), and 4.08 (2 H, m, CHBr).

Solvents.—DMF (Koch–Light; puriss.) was vacuum distilled using a Widmer column and g.l.c. analysis of the product showed it to contain <300 p.p.m. water. Ammonia was taken as a gas from the commercial cylinder (B.O.C. pure ammonia) and condensed over sodium in a stainless steel reservoir from which it was distilled into a vacuum line as required.

Electrolytes.—Tetrabutylammonium tetrafluoroborate was prepared by published methods.[18] Potassium bromide (B.D.H.; AnalaR) was recrystallised from thrice distilled water, dried at 120 °C, ground finely, and stored in the oven at 120 °C.

Reference Electrodes.—All electrode potentials are quoted with respect to the experimental reference electrodes which were, for DMF and ammonia solutions respectively, $Ag|AgNO_3$ (1.0×10^{-3}M), $MgCl_2$ (10×10^{-3}M), 0.4M-TBAF, DMF|| and $Pb|Pb(NO_3)_2$ (1.0×10^{-3}M), KBr (0.5M), liquid NH_3||.

Working Electrodes.—Twice distilled mercury was used for the dropping mercury electrode, the mercury pool, and the amalgamated copper electrode. Vitreous carbon electrodes

were in the form of short rods (Le Carbone) and gold and platinum indicator electrodes were wires (Johnson-Matthey). In all preparative cells, the working and counter electrodes were parallel and facing one another and the back of the working electrode was disabled by insulation so that non-uniformity of electrode potential was minimised. Solid metals were in the form of sheets.

Co-solvents.—Limited solubility of compounds (2) in liquid ammonia at −40 °C, the temperature used for all experiments with that solvent, required the use of co-solvents. After investigating diethyl ether and butylamine, we finally chose tetrahydrofuran (THF) as most suitable. The reagent (B.D.H.) was refluxed for 5 h with calcium hydride (B.D.H.) to remove water and peroxides and was then distilled into a sealed vessel for transfer to the electrochemical cell.

Product Analysis.—Analysis was performed using g.l.c. After electrolyses of DMF solutions the catholytes were injected without work-up. Two columns were used, the first to determine all the components of the mixture and the second to find the proportions of *cis*- and *trans*-hexenes. Column 1 was 10% Carbowax 20M on Phase-sep W 60—80 mesh in 1.5 m × 4 mm glass in Pye 105 with flame detection (f.i.d.) at 138 °C using N_2 carrier, flow rate 50 cm^3 min^{-1}. Column 2 was 33% 1,2-dihydroxyethane saturated with $AgNO_3$ on Embacel 60—100 mesh, acid-washed, in 2.0 m × 4 mm glass in Pye 105 with f.i.d. at 21 °C using N_2, flow rate 30 cm^3 min^{-1}.[19]

Following experiments involving ammonia as the principal solvent, the cell temperature was allowed to rise and ammonia gas was allowed to escape overnight, leaving the reaction mixture dissolved in the THF co-solvent which was then analysed. In all, four different g.l.c. columns were involved. Column 1 was used as previously to examine the overall product distribution following reactions of (1). The corresponding preliminary studies of reaction mixtures resulting from reductions of (2) made use of columns 3 and 4. Column 3 was 20% Tween 80 on Diatoport W 80—100 mesh in 6.0 ft × ¼ in stainless steel in F & M 810, temperature programmed from 78 (8 min) to 150 °C at 60 °C min^{-1} using N_2, flow rate 40 cm^3 min^{-1}. Column 4 was 10% GESE 52 on Diatoport S 80—100 mesh in 6 ft × ¼ in stainless steel in F & M 810, temperature programmed from 45 (13 min) to 205 °C at 10 °C min^{-1} using N_2, flow rate 30 cm^3 min^{-1}. As previously described distinction between *cis*- and *trans*-alkenes (3) and (4) made use of column 2.

In addition to analyses based upon identity of retention times of sample components and the respective standard materials, preparative g.l.c. was used to isolate the fractions of the separated isomers of (3) and (4) for mass spectrometric examination. The column used, 5, was similar to column 2 except that stainless steel tubing was used and the F & M 810 chromatograph was used with its thermal conductivity detector (He carrier gas) so that samples could be collected in micro-traps.

Appendix 1.

Estimations of Strain Energies of Reactant Rotamers.—In order to interpret the experimental results it was necessary to estimate relative stabilities of possible conformations of the vicinal dibromides (1) and (2). Strain energies consist of contributions from various intramolecular interactions: van der Waals, dipole–dipole, and repulsions between bonding electrons. These effects cause distortions in bond lengths and angles which give rise to further contributions. The method of ' molecular mechanics ' is used to quantify these various

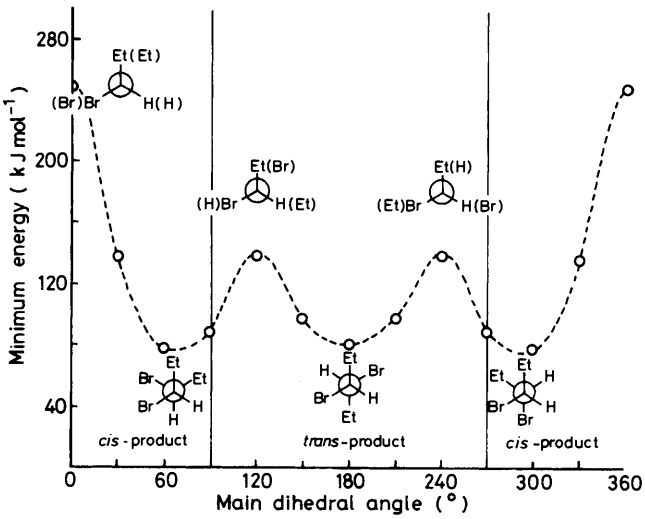

Figure 5. Minimum conformational energies (van der Waals contributions only) of *meso*-3,4-dibromohexane as a function of the main dihedral angle ∠ BrCCBr

Table 3. Data used in the molecular mechanics calculations

Atom X	C	H	Br
C–X bond length (nm)	0.152	0.1113	0.196
van der Waals radius of X (nm)	0.185	0.146	0.204
Hardness parameter of X (kJ mol^{-1})	0.20	0.31	1.26

phenomena.[20,21] The approach used in the present work is a very much simplified application of the molecular mechanics method aimed at producing qualitative, or at best semi-quantitative, estimates of the relative energies of molecules (1) and (2) as functions of the dihedral angle between the two C–Br bonds. The only terms to be considered during the calculations were those arising from van der Waals interactions. Terms were summed for every pair of atoms separated by more than two bonds. For a chosen value of the main dihedral angle, all other dihedral angles were adjusted in order to obtain a minimum in the total van der Waals strain energy. The neglect of dipolar interactions and torsional terms will no doubt have introduced errors into the calculations. Furthermore ignoring bond bending and stretching which normally relieve some of the primary strain will have had the effect of exaggerating strain energies. Thus values of a few hundred kJ mol^{-1} have been obtained for less stable conformations. Nevertheless the exercise is considered worthwhile as a means of estimating relative stabilities of the more stable arrangements. Quantitative application of the results of the calculations, for example to calculate equilibrium constants for *anti–gauche* equilibria, would be wholly inappropriate as the energy-minimisation process has caused configurational entropy factors to be neglected.

The basis for the calculations was the Hill equation (1).[22]

$$E_v = \varepsilon\{-2.25\,A^{-6} + 8.28 \times 10^5 \exp(-A/0.0736)\} \quad (1)$$

Here, E_v is the van der Waals interaction energy between a pair of atoms whose nuclei are separated by a distance A, measured in units of the sum of the van der Waals radii of the two atoms. ε is the ' hardness parameter ' of the pair, calculated as the geometric mean of the hardness parameters of the individual atoms. Following Meyer,[23] who has applied

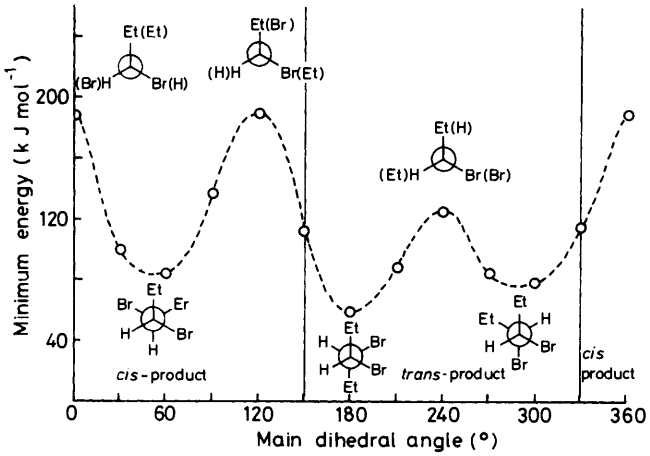

Figure 6. Minimum conformational energies (van der Waals contributions only) of DL-3,4-dibromohexane as a function of the main dihedral angle ∠EtCCEt

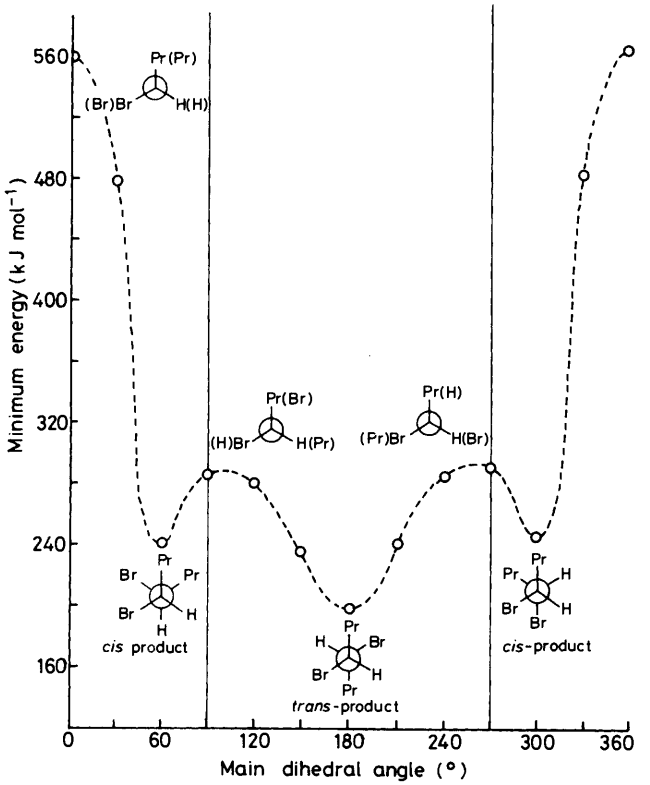

Figure 7. Minimum conformational energies (van der Waals contributions only) of *meso*-2,5-dimethyl-3,4-dibromohexane as a function of the main dihedral angle ∠BrCCBr

Allinger's method of calculation to various other organic bromides, we have used, as the basis for our calculations, the data of Table 3. Bond angles were supposed tetrahedral with the exception of those involving C-3 and -4 to which bromine atoms are bonded (∠CCBr 108.8°, ∠HCBr 105.6°, ∠CCH 109.5°). Calculations were performed interactively, using an Apple II Plus computer as a programmable calculator, after selecting approximate minimum-energy arrangements by means of molecular models; a variation method, involving rotations about all bonds, was then applied to obtain the final minimisation. The results of the calculations are presented in Figures 5—8 and Tables 4—7.

In the case of compound (2), the results of our calculations find general support from ^{1}H n.m.r. studies. In that conform-

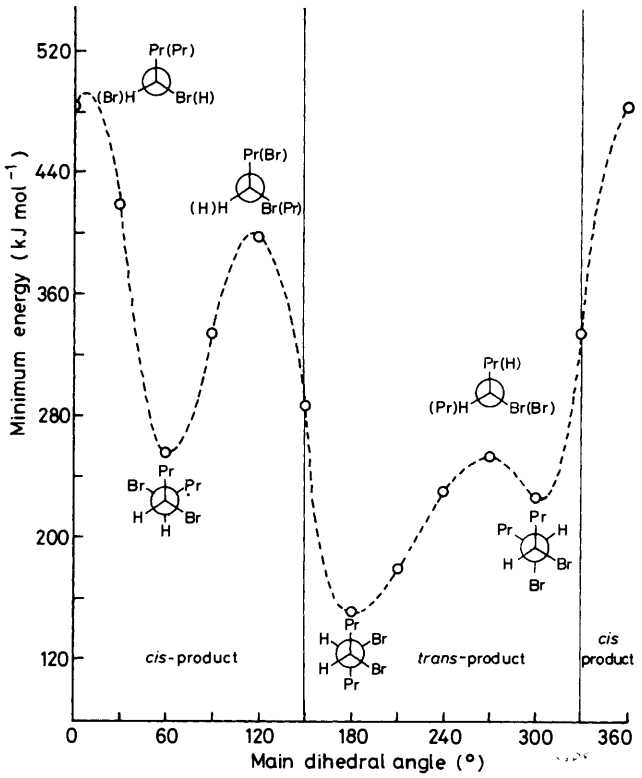

Figure 8. Minimum conformational energies (van der Waals contributions only) of DL-2,5-dimethyl-3,4-dibromohexane as a function of the main dihedral angle ∠Pr^{i}CCPr^i

Table 4. Strain energies arising from van der Waals interactions in *meso*-3,4-dibromohexane

Dihedral angle (°) about C-3–C-4 bond	Dihedral angle (°) about C-2–C-3 bond *	Dihedral angle (°) about C-4–C-5 bond *	Strain energy (kJ mol^{-1})
0	179.5	179.5	248.5
30	186	170	137
60	186	157	78
90	161	161	88
120	179	177	131
150	192	168	98
180	180.5	180.5	80
210	168	192	98
240	177	179	131
270	161	161	88
300	157	186	78
330	170	186	137

* Angles adjusted to correspond to minimum strain energy.

Table 5. Strain energies arising from van der Waals interactions in DL-3,4-dibromohexane

Dihedral angle (°) about C-3–C-4 bond	Dihedral angle (°) about C-4–C-5 bond *	Dihedral angle (°) about C-2–C-3 bond *	Strain energy (kJ mol^{-1})
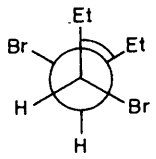	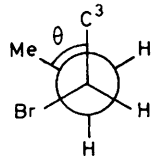	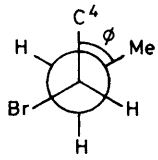	
0	192.3	167.7	188.6
30	194.5	165.5	100.5
60	201	159	84.8
90	165	195	136.8
120	180.4	179.6	190.2
150	199.5	160.5	113.0
180	205.5	154.5	59.6
210	187	173	89.0
240	181.5	178.5	126.4
270	202	158	85.0
300	168	192	78.5
330	173	187	114.8

* Angles adjusted to correspond to minimum strain energy.

Table 6. Strain energies arising from van der Waals interactions in *meso*-2,5-dimethyl-3,4-dibromohexane

Dihedral angle (°) about C-3–C-4 bond	Dihedral angle (°) about C-2–C-3 bond *	Dihedral angle (°) about C-4–C-5 bond *	Strain energy (kJ mol^{-1})
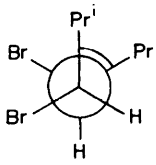	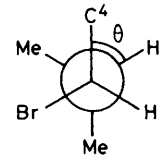	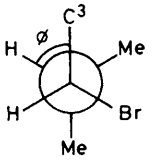	
0	38.5	−34	559
30	4.5	−18	478
60	−14	6	241
90	−57	−56	286
120	−47	−48	280.5
150	−58	64	237
180	28	28	196
210	64	−58	237
240	−48	−47	280.5
270	−56	−57	286
300	6	−14	241
330	−18	4.5	478
360	−34	38.5	559

* Angles adjusted to correspond to minimum strain energy.

ation of *meso*-(2) which we predict to be most stable (*anti*-arrangement at the central C-3–C-4 bond and $\theta = \varphi = 28°$), the dihedral angles existing between the bromomethine hydrogens and the vicinal isopropyl hydrogens are 90°. Correspondingly, the ^{1}H n.m.r. coupling constant should be minimal and, indeed, a high-resolution spectrum [24] indicates that a small coupling (*ca.* 2 Hz) exists for the bromomethine proton resonance. By contrast, the theoretically predicted most stable conformer of DL-(2) has a value of *ca.* 180° for the dihedral

Table 7. Strain energies arising from van der Waals interactions in DL-2,5-dimethyl-3,4-dibromohexane

Dihedral angle (°) about C-3–C-4 bond	Dihedral angle (°) about C-2–C-3 bond *	Dihedral angle (°) about C-4–C-5 bond *	Strain energy (kJ mol^{-1})
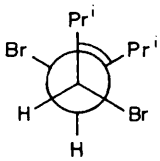	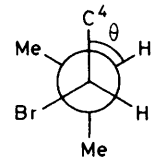	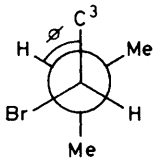	
0	−36	36	484
30	−50	50	419
60	−8	8	256
90	−26.5	−26.5	334
120	−46	46	398
150	−62	62	287
180	−62	62	152
210	−53	53	180
240	−41	41	230
270	62	−62	254
300	12	−12	227
330	55.4	−55.4	336

* Angles adjusted to correspond to minimum strain energy.

angle between the bromomethine and the adjacent isopropyl protons and the resulting large coupling constant was manifested as a multiplet in the n.m.r. spectrum. Clearly free rotation about the C-3–C-4 bond is restricted in both isomers. Indeed, the splitting of the spectrum due to the methyl hydrogens into *two* 6 H doublets for each isomer indicates that rotations about the adjacent C-2–C-3 and C-4–C-5 bonds are also hindered.

Appendix 2.

Calculations of Distances of Heterogeneous Electron Transfer.—When cathodic processes are performed at values of electrode potential much more negative than $E_{\frac{1}{4}}$ then the rate of the heterogeneous process is controlled solely by the rate of mass transfer of the reactant species to the electrode. In the limit, the activation energy for the charge-transfer event tends to zero; every reactant particle which reaches the vicinity of the electrode is immediately reduced. The heterogeneous reaction can be treated as a homogeneous process in which the first-order rate constant increases as the reactant particle approaches the electrode surface; the rate constant is the product of a frequency factor (kT/h) and a term which expresses the probability of electron tunnelling from the electrode to the reactant.[25] This latter term must depend upon the thickness and shape of the potential barrier to tunnelling.

$$\text{Rate} = c(kT/h)f(x) = ck_1'f(x) \qquad (2)$$

In general, $f(x)$ will not be a simple function but, for purposes of semi-quantitative argument, we can approximate the shape of the potential barrier to a rectangle. In equation (3), c is

$$f(x) = \exp -\{4\pi x[2M(U - E)]^{\frac{1}{2}}/h\} = \exp -k_2x \qquad (3)$$

concentration of reactant, $U - E$ is the height of the barrier, M is the mass of the electron, T is temperature, x is distance separating the electrode and the reactant and k and h are the constants of Boltzmann and Planck respectively.

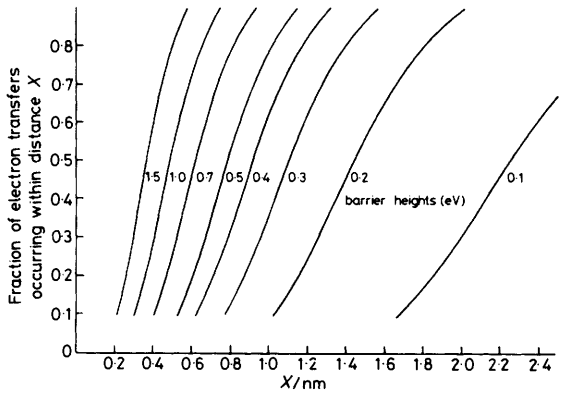

Figure 9. Distribution of electron-transfer distances for various barrier heights, when the reaction rate is completely controlled by mass-transfer of the reactant. The assumed concentration gradient within the diffusion layer is 1.0×10^5 mol m^{-4}

In the steady state the reaction rate will be balanced by the rate of diffusion, supposed semi-infinite linear, of the reactant [equation (4)]. D is the diffusion coefficient of the reactant.

$$D\mathrm{d}^2c/\mathrm{d}x^2 = k_1'c\cdot\exp -k_2x \qquad (4)$$

Equation (4) can be solved by making the substitution (5).

$$v = 2(k_1'^{\frac{1}{2}}/k_2)\cdot\exp(-k_2x/2) \qquad (5)$$

The solution is in terms of modified Bessel functions $I_0(v)$ and $K_0(v)$. Differentiation affords expression (7) for the

$$c = AI_0(v) + BK_0(v) \qquad (6)$$

concentration gradient. Arbitrary constants A and B were

$$\begin{aligned}\mathrm{d}c/\mathrm{d}x &= -k_2v\{A\cdot I_0'(v) + B\cdot K_0'(v)\}/2 \\ &= k_2v\{B\cdot K_1(v) - A\cdot I_1(v)\}/2 \end{aligned} \qquad (7)$$

evaluated by setting the concentration gradient in the diffusion layer (c_{bulk}/δ) and by recognising that at $x = 0$, $\mathrm{d}c/\mathrm{d}x$ is zero.

In this way, calculations have been carried out for various barrier heights and mass-transfer fluxes, of distributions of concentration near to the electrode surface and hence the distribution of distances over which electron transfer occurs has been determined. The calculations, which were performed with an Apple II Plus computer, made use of published polynomial approximations to the modified Bessel functions I_0, I_1, K_0, and K_1.[26] Results are presented in Figure 9. There it is shown that for a rectangular barrier of height 1.0 eV fewer than half the electron transfers take place over distances greater than 0.5 nm. However, for barrier heights below 0.3 eV, half of the electron transfers occur over distances in excess of 1.1 nm. It can be argued that, at electrode potentials approaching those at which solvated electrons can be generated, barrier heights become low and, in consequence, electron transfers to diffusion-controlled species are expected to involve relatively large tunnelling distances.

Acknowledgements

The S.E.R.C. supported this work as part of a CASE project. We thank Dr. R. S. Johnson for advice on the solution of the differential equation (Appendix 2).

References

1 M. Stackelberg and W. Stracke, *Z. Elektrochem.*, 1949, **53**, 118.
2 H. R. Koch and M. G. McKeon, *J. Electroanal. Chem.*, 1971, **30**, 331.
3 J. Casanova and H. R. Rogers, *J. Org. Chem.*, 1974, **39**, 2408.
4 J. Zavada, J. Krupicka, and J. Sicher, *Collect. Czech. Chem. Commun.*, 1963, **28**, 1664.
5 (*a*) A. J. Klein and D. H. Evans, *J. Am. Chem. Soc.*, 1979, **101**, 757; (*b*) K. M. O'Connell and D. H. Evans, *ibid.*, 1983, **105**, 1473.
6 L. G. Feoktistov and M. M. Gol'din, *Sov. Electrochem.*, 1968, **4**, 435.
7 M. M. Gol'din, L. G. Feoktistov, A. P. Tomilov, and K. M. Smirnov, *J. Gen. Chem. USSR*, 1972, **42**, 2552.
8 L. G. Feoktistov and M. M. Goldin, *J. Gen. Chem. USSR*, 1973, **43**, 519.
9 W. Adam and J. Arce, *J. Org. Chem.*, 1972, **37**, 507.
10 J. F. Garst, J. A. Pacifici, V. D. Singleton, M. E. Ezzel, and J. I. Morris, *J. Am. Chem. Soc.*, 1975, **97**, 5242.
11 P. J. Elving, I. Rosenthal, and A. J. Martin, *J. Am. Chem. Soc.*, 1955, **77**, 5218.
12 H. Lund and E. Hobolth, *Acta Chem. Scand., Ser. B*, 1976, **30**, 895.
13 G. Faita, M. Fleischmann, and D. Pletcher, *J. Electroanal. Chem.*, 1970, **25**, 455.
14 T. H. Teherani, W. J. Peer, J. J. Lagowski, and A. J. Bard, *J. Am. Chem. Soc.*, 1978, **100**, 7768.
15 O. R. Brown, H. R. Thirsk, and B. Thornton, *Electrochim. Acta*, 1971, **16**, 495.
16 C. G. Schmitt and C. E. Boord, *J. Am. Chem. Soc.*, 1932, **54**, 751.
17 W. G. Young, Z. Jasaitis, and L. Levanas, *J. Am. Chem. Soc.*, 1937, **59**, 403.
18 C. R. Witschonke and C. A. Kraus, *J. Am. Chem. Soc.*, 1947, **69**, 2472; E. J. del Rosario and J. E. Lind, *J. Phys. Chem.*, 1966, **70**, 2876.
19 E. Gil-Av, J. Herling, and J. Shabtai, *J. Chromatogr.*, 1958, **1**, 508; 1959, **2**, 406; 1963, **11**, 32.
20 N. L. Allinger, *Adv. Phys. Org. Chem.*, 1976, **13**, 1.
21 E. L. Eliel, N. L. Allinger, S. J. Angyal, and G. A. Morrison, 'Conformational Analysis,' Wiley, New York, 1965.
22 T. L. Hill, *J. Chem. Phys.*, 1948, **16**, 399.
23 A. Y. Meyer and O. Ohmichi, *J. Mol. Struct.*, 1981, **73**, 145.
24 H. B. Thompson and W. N. Opdycke, *J. Org. Chem.*, 1981, **46**, 1786.
25 V. G. Levich, 'Physical Chemistry,' eds. H. Eyring, D. Henderson, and W. Jost, Academic Press, New York, 1970, vol. IXB, p. 898.
26 M. Abramowitz and I. A. Segun, 'Handbook of Mathematical Functions,' Dover Press, New York, 1965, p. 378.

Received 24*th June* 1983; *Paper* 3/1082